



SPE 106254

Operator Based Multiscale Method for Compressible Flow

H. Zhou, SPE and H. A. Tchelepi, SPE, Stanford University

Copyright 2007, Society of Petroleum Engineers

This paper was prepared for presentation at the 2007 SPE Reservoir Simulation Symposium held in Houston, Texas, U.S.A., 26-28 February 2007.

This paper was selected for presentation by an SPE Program Committee following review of information contained in an abstract submitted by the author(s). Contents of the paper, as presented, have not been reviewed by the Society of Petroleum Engineers and are subject to correction by the author(s). The material, as presented, does not necessarily reflect any position of the Society of Petroleum Engineers, its officers, or members. Papers presented at SPE meetings are subject to publication review by Editorial Committees of the Society of Petroleum Engineers. Electronic reproduction, distribution, or storage of any part of this paper for commercial purposes without the written consent of the Society of Petroleum Engineers is prohibited. Permission to reproduce in print is restricted to an abstract of not more than 300 words; illustrations may not be copied. The abstract must contain conspicuous acknowledgment of where and by whom the paper was presented. Write Librarian, SPE, P.O. Box 833836, Richardson, Texas 75083-3836 U.S.A., fax 01-972-952-9435.

Abstract

Recently, multiscale methods have been developed for accurate and efficient numerical solution of large-scale heterogeneous reservoir problems. A scalable and extendible Operator Based Multiscale Method (OBMM) is described here. OBMM is cast as a general algebraic framework of the multiscale method. It is very natural and convenient to incorporate more physics in OBMM for multiscale computation.

In OBMM, two multiscale operators are constructed: prolongation and restriction. The prolongation operator can be constructed by assembling basis functions, and the specific form of the restriction operator depends on the coarse-scale discretization formulation (e.g., finite-volume or finite-element). The coarse-scale pressure equation is obtained algebraically by applying the prolongation and restriction operators on the fine-scale flow equations. Solving the coarse-scale equation results in a high quality coarse-scale pressure. The fine scale pressure can be reconstructed by applying the prolongation operator to the coarse-scale pressure. A conservative fine-scale velocity field is then reconstructed to solve the transport equation.

As an application example, we study multiscale modeling of compressible flow. We show that the extension of modeling from incompressible to compressible flow is really straightforward for OBMM. No special treatment for compressibility is required. The efficiency of multiscale methods over stan-

ard fine-scale methods is retained by OBMM. The accuracy of OBMM is demonstrated by several challenging cases including highly compressible multiphase flow in a strongly heterogeneous permeability field (SPE 10).

Introduction

The accuracy of simulating subsurface flow relies strongly on the detailed geologic description of the porous formation. Formation properties such as porosity and permeability typically vary over many scales. As a result, it is not unusual for a detailed geologic description to require $O(10^7) - O(10^8)$ grid cells. However, this level of resolution is far beyond the computational capability of state-of-the-art reservoir simulators ($O(10^6)$ grid cells). Moreover, some applications need to run many reservoir simulations (e.g., history matching, sensitivity analysis and stochastic simulation). Thus, it is necessary to have an efficient and accurate computational method to study these highly detailed models.

The multiscale method is very promising due to its ability to resolve fine-scale information accurately without direct solution of the global fine-scale equations. Recently, there has been increasing interest in multiscale methods. Hou and Wu⁴ proposed a multiscale finite-element method (MsFEM) that captures the fine-scale information by constructing special finite element basis functions within each element. However, the reconstructed fine-scale velocity is not conservative. Later, Chen and Hou proposed a conservative mixed finite-element multiscale method. Another multiscale mixed finite-element method has been presented by Arbogast¹ and Arbogast and Bryant². Numerical Green functions were used to resolve the fine-scale information, which are then coupled with coarse-scale operators to obtain the global solution. These methods considered incompressible flow in heterogeneous porous media where the flow equation is elliptic.

A multiscale finite-volume method (MsFVM) was proposed by Jenny, Lee and Tchelepi⁵ for heterogeneous elliptic problems. They employed two sets of basis functions — dual and primal. The dual basis functions are identical to those of Hou

and Wu⁴, while the primal basis functions are obtained by solving local elliptic equations with Neumann boundary conditions calculated from the dual basis functions.

Existing multiscale methods¹⁻⁵ deal with the incompressible flow problem only. However, compressibility will be significant if a gas phase is present. Gas has a large compressibility which is usually a strong function of pressure. Therefore, there can be significant spatial compressibility variations in the reservoir, and this is a challenge for multiscale modeling. Very recently, Lunati and Jenny considered compressible multiphase flow⁸ in the framework of MsFVM. They proposed three models to account for the effects of compressibility. Using those models, compressibility effects were represented in the coarse-scale equations and the reconstructed fine-scale fluxes according to the magnitude of compressibility.

Motivated to construct a multiscale framework that can deal with compressible multiphase flow in highly detailed heterogeneous models, we developed an operator based multiscale method (OBMM). The OBMM algorithm is composed of four steps: (1) constructing the prolongation and restriction operators, (2) assembling and solving the coarse-scale pressure equations, (3) reconstructing the fine-scale pressure and velocity fields, and (4) solving the fine-scale transport equations.

OBMM is a general algebraic multiscale framework for compressible multiphase flow in heterogeneous reservoirs. This algebraic framework can also be extended naturally from structured to unstructured grids. Moreover, the OBMM approach may be used to employ multiscale solution strategies in existing simulators with a relatively small investment.

Operator Based Multiscale Method

In this section, we describe the operator based multiscale method (OBMM) for the two-phase flow problem. We show that, for incompressible flow, OBMM is identical to the original MsFVM⁵. The effects of compressibility are taken into account naturally when constructing the coarse-scale operators. The basis functions and reconstructed fine-scale fluxes also contain the compressibility effects. The overall algorithm to solve coupled flow and transport problems with the OBMM framework is described, and adaptive computation of the basis functions is discussed.

Model Equations. We consider immiscible two-phase flow in porous media. Extension to three-phase flow is straightforward. Gravity and capillarity are neglected here. The governing equations are the mass conservation equations of the two phases,

$$\begin{aligned} \frac{\partial(\phi b_l)}{\partial t} - \nabla \cdot (b_l u_l) &= q_l, \\ u_l &= -\lambda_l \nabla p, \\ \lambda_l &= \frac{k k_{r_l} b_l}{\mu}, \end{aligned} \quad (1)$$

where $l = 1, 2$ denotes the two phases; b_l is the inverse of the phase formation-volume factor, which is defined as the ratio of density at reservoir conditions to density at standard conditions; u_l is the phase volumetric flux at reservoir condition; q_l is the source term; λ_l is the phase mobility; k_{r_l} is the phase relative

permeability; ϕ and k are the porosity and absolute permeability of porous media.

Because multiscale methods are usually applied only to the flow problem (pressure equation), the flow and transport problems should be decoupled first. Thus, the flow and transport equations are solved sequentially using either an IMPES (Implicit Pressure Explicit Saturation)⁶ or a sequential fully implicit (SFI)⁷ method. Here we adopt the sequential fully implicit approach. The linearized discrete pressure equation can be obtained from Eq.1 through simple algebraic manipulation. The semi-discrete equation for iteration $\nu + 1$ at time step $n + 1$ is

$$\begin{aligned} C \frac{p^{\nu+1} - p^\nu}{\Delta t} - \alpha_1^\nu \nabla \cdot (b_1^\nu \lambda_1^\nu \nabla p^{\nu+1}) - \alpha_2^\nu \nabla \cdot (b_2^\nu \lambda_2^\nu \nabla p^{\nu+1}) \\ = RHS, \end{aligned} \quad (2)$$

where,

$$\begin{aligned} \alpha_1^\nu &= \frac{1}{b_1^\nu}, \quad \alpha_2^\nu = \frac{1}{b_2^\nu}, \\ C &= \left(\frac{\partial \phi}{\partial p} - \phi^n (b_1^n S_1^n \frac{\partial \alpha_1}{\partial p} + b_2^n S_2^n \frac{\partial \alpha_2}{\partial p}) \right. \\ &\quad \left. + \Delta t \frac{\partial(\alpha_1 q_1 + \alpha_2 q_2)}{\partial p} \right)^\nu, \\ RHS &= -\frac{\phi^\nu}{\Delta t} + \frac{\phi^n}{\Delta t} (\alpha_1^\nu b_1^n S_1^n + \alpha_2^\nu b_2^n S_2^n) - (\alpha_1 q_1^\nu + \alpha_2 q_2^\nu). \end{aligned} \quad (3)$$

Given a fine-scale problem, Eq.2 can be written in matrix form as

$$(\mathbf{T}_f - \mathbf{C}_f) \mathbf{p}_f = \mathbf{r}_f, \quad (4)$$

where \mathbf{T}_f is the fine-scale transmissibility matrix associated with the flow part, \mathbf{C}_f is the fine-scale compressibility matrix associated with the accumulation part, \mathbf{p}_f denotes the fine-scale pressure vector, and \mathbf{r}_f is the fine-scale right hand side vector.

The linearized discrete form of the transport equation for phase 1 is

$$\begin{aligned} \frac{\phi^{\nu+1} b_1^{\nu+1} S_1^{\nu+1} - \phi^n b_1^n S_1^n}{\Delta t} \\ = \nabla \cdot \left\{ \left[b_1^{\nu+1} (f_1^\nu + \frac{\partial f_1}{\partial S_1})^\nu (S_1^{\nu+1} - S_1^\nu) \right] \mathbf{u}_T^{\nu+1} \right\} - q_1, \end{aligned} \quad (5)$$

where f_1 is the fractional flow of phase 1, and \mathbf{u}_T is the total velocity.

Prolongation Operator. The multiscale prolongation operator, \mathcal{P} , is defined as the mapping from coarse-scale pressure to fine-scale pressure, i.e.,

$$\mathbf{p}_f = \mathcal{P} \mathbf{p}_c, \quad (6)$$

where \mathbf{p}_c denotes the cell-center coarse-scale pressure. Hou and Wu⁴ used a set of specially constructed basis functions

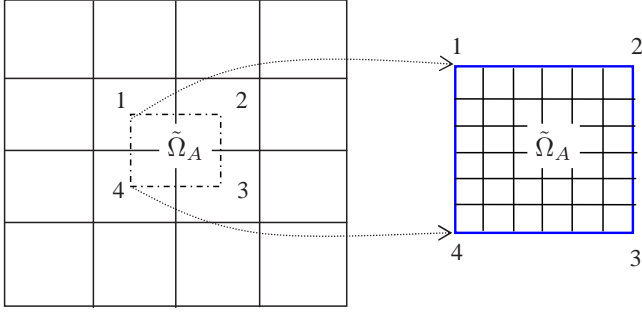


Figure 1: Two-dimensional multiscale grid with a typical dual control volume. The enlarged dual control volume shows the underlying fine grid.

to relate the fine and coarse pressures. Although their study was for the incompressible flow (elliptic) problem, we have found that these basis functions also work for parabolic problems (e.g., compressible flow). The construction of the basis functions for Eq.1 is discussed below.

Considering a two dimensional multiscale grid as shown in Fig.1, the whole physical domain is partitioned into disjoint coarse blocks (primal coarse blocks) and each coarse block is further partitioned into fine cells. A set of dual coarse blocks is defined by connecting the centers of each coarse block. The idea of the dual-coarse grid offers great advantages in constructing accurate and conservative fluxes on the primal coarse grid⁵.

A basis function associated with coarse node i ($i = 1, \dots, 4$) in dual block $\tilde{\Omega}_A$ is obtained by solving the elliptic part of Eq.1,

$$\begin{aligned} \alpha_1^\nu \nabla \cdot (b_1^\nu \lambda_1^\nu \nabla \phi_A^i) + \alpha_2^\nu \nabla \cdot (b_2^\nu \lambda_2^\nu \nabla \phi_A^i) &= 0 \quad \text{in } \tilde{\Omega}_A, \\ \alpha_1^\nu \frac{\partial}{\partial x_t} \left(b_1^\nu \lambda_1^\nu \frac{\partial \phi_A^i}{\partial x_j} \right)_t + \alpha_2^\nu \frac{\partial}{\partial x_t} \left(b_2^\nu \lambda_2^\nu \frac{\partial \phi_A^i}{\partial x_j} \right)_t &= 0 \quad \text{on } \partial \tilde{\Omega}_A, \\ \phi_A^i(\mathbf{x}_j) &= \delta_{ij}, \end{aligned} \quad (7)$$

where subscript t denotes the component tangential to the boundary, and j denotes any coarse node in $\tilde{\Omega}_A$ ($j = 1, \dots, 4$). Let K be the global index of a coarse node, $i_{K,A}$ be the local index of node K in dual block $\tilde{\Omega}_A$, and \mathcal{D}_K the set of dual blocks intersected by node K . For Cartesian grid, the number of elements in \mathcal{D}_K is 2^d , where d is the number of dimensions. Using a global point of view, a basis function can be written as

$$\phi_K = \sum_{\tilde{\Omega}_A \in \mathcal{D}_K} \phi_A^{i_{K,A}} \quad (8)$$

The multiscale prolongation operator, \mathcal{P} , is an $n \times N$ matrix, where n is the number of global fine nodes and N is the number of global coarse nodes. Let k denote a fine node and K a coarse node. Then one has

$$\mathcal{P}_{k,K} = \phi_K(\mathbf{x}_k) \quad (9)$$

Restriction Operator. Plugging Eq.6 into Eq.4, one obtains,

$$(\mathbf{T}_f - \mathbf{C}_f) \mathcal{P} \mathbf{p}_c = \mathbf{r}_f. \quad (10)$$

The significance of Eq.10 is that its unknowns are coarse-scale pressures. We need to apply a restriction operator, \mathcal{R} , that provides a mapping from fine to coarse space. So we write

$$\mathcal{R}(\mathbf{T}_f - \mathbf{C}_f) \mathcal{P} \mathbf{p}_c = \mathcal{R} \mathbf{r}_f, \quad (11)$$

or,

$$(\mathbf{T}_c - \mathbf{C}_c) \mathbf{p}_c = \mathbf{r}_c, \quad (12)$$

where $\mathbf{T}_c, \mathbf{C}_c, \mathbf{r}_c$ are the coarse-scale counterparts of $\mathbf{T}_f, \mathbf{C}_f, \mathbf{r}_f$, and are defined as

$$\begin{aligned} \mathbf{T}_c &= \mathcal{R} \mathbf{T}_f \mathcal{P} \\ \mathbf{C}_c &= \mathcal{R} \mathbf{C}_f \mathcal{P} \\ \mathbf{r}_c &= \mathcal{R} \mathbf{r}_f. \end{aligned} \quad (13)$$

Eq.12 is the coarse-scale equation we need to solve.

The restriction operator, \mathcal{R} , maps the fine-scale discretization equations into the coarse scale. It is not unique. The specific choice for \mathcal{R} depends on the discretization scheme (e.g., finite element or finite volume). We denote a fine-scale conservative equation by E . A finite volume formulation starts with

$$\int_{\Omega_k} E dV = 0 \quad (\forall \text{ fine cell } \Omega_k, k = 1, \dots, n). \quad (14)$$

A coarse-scale finite volume formulation requires

$$\int_{\Omega_K} E dV = 0 \quad (\forall \text{ coarse block } \Omega_K, K = 1, \dots, N). \quad (15)$$

Comparing Eq.14 and Eq.15, it is clear that Eq.15 can be obtained by summing Eq.14 for all the fine cells inside a coarse block K , i.e.,

$$\int_{\Omega_K} E dV = \sum_{\Omega_k \in \Omega_K} \int_{\Omega_k} E dV. \quad (16)$$

The summation in Eq.16 can be represented by the restriction operator, \mathcal{R} , as follows,

$$\mathcal{R}_{K,k} = \begin{cases} 1 & \text{if } \Omega_k \subset \Omega_K \\ 0 & \text{otherwise} \end{cases} \quad (K = 1, \dots, N; k = 1, \dots, n). \quad (17)$$

It is also important to note that the restriction operator does not depend on the detailed discretization scheme (i.e., backward difference or central difference, etc.) and thus is general for a given formulation.

For a Galerkin-type finite element method, the coarse-scale equation may be written as

$$\int_{\Omega_K} \phi_M E dV = 0 \quad (K, M = 1, \dots, N) \quad (18)$$

and one can show that \mathcal{R} takes the following form

$$\mathcal{R} = \mathcal{P}^T. \quad (19)$$

Zhou⁹ provides a detailed treatment for finite-element based multiscale formulations.

Coarse-Scale Operators. Given the prolongation and restriction operators defined above, the coarse-scale system, Eq.12, can be constructed. We try to shed some light on the physical meaning of the coarse-scale operators. The focus is on OBMM using the finite-volume formulation (i.e., \mathcal{R} given by Eq.17).

To make the analysis easier, consider a one-dimensional problem. Fig.2 shows the grid with coarse blocks $K-1, K, K+1$, fine cells $k-4, \dots, k+4$. We first look at the incompressible

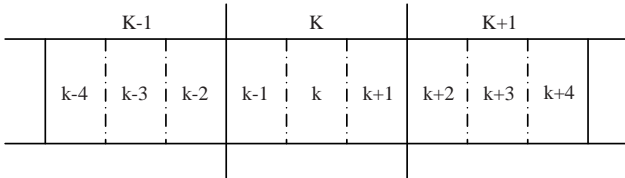


Figure 2: One-dimensional multiscale grid

case where Eq.1 becomes

$$\nabla \cdot (\lambda_t \nabla p) = q_t, \quad (20)$$

where, $\lambda = \lambda_1 + \lambda_2$ is the total mobility, and q_t is the total source term. Using a central difference scheme in the fine-scale discretization, the OBMM algorithm gives three non-zeros elements for the K^{th} row of the coarse-scale transmissibility matrix, i.e.,

$$\begin{aligned} T_{cK,K-1} &= -\frac{\lambda_{k-3/2}}{\Delta x} (\phi_{K-1}(x_{k-1}) - \phi_{K-1}(x_{k-2})), \\ T_{cK,K} &= -\frac{\lambda_{k-3/2}}{\Delta x} (\phi_K(x_{k-1}) - \phi_K(x_{k-2})) \\ &\quad + \frac{\lambda_{k+3/2}}{\Delta x} (\phi_K(x_{k+2}) - \phi_{K-1}(x_{k+1})), \quad (21) \\ T_{cK,K+1} &= -\frac{\lambda_{k+3/2}}{\Delta x} (\phi_{K+1}(x_{k+2}) - \phi_{K+1}(x_{k+1})). \end{aligned}$$

These coarse-scale operators are exactly the same as the effective coarse-grid transmissibility constructed by Jenny et al.⁵ For example, from Eq.21, $T_{cK,K-1}$ is the flux across the interface of coarse blocks $K-1$ and K with respect to a unit pressure at node $K-1$.

Compressibility is taken into account in the basis functions, Eq.7, and in constructing the coarse-scale transmissibility and compressibility matrices, Eq.13. The fine-scale fluxes represented by \mathbf{T}_f contain compressibility effects, and OBMM gives the coarse-scale fluxes by summing up the fine-scale fluxes in a coarse block. Therefore, the effective transmissibility constructed by OBMM accounts for compressibility of the flow. The coarse-scale compressibility matrix in Eq.13 is obtained by redistributing accumulation terms in the coarse grid according to the underlying fine-scale accumulation terms. By construction, the scheme is conservative on both the fine and coarse scales.

Fine-scale Velocity. The coarse-scale pressure, \mathbf{p}_c , is obtained from Eq.12 and then the so-called dual fine-scale pressure, \mathbf{p}_d , is reconstructed by

$$\mathbf{p}_d = \mathcal{P}\mathbf{p}_c. \quad (22)$$

```

 $\nu_p = 1; \nu_s = 1; p^{\nu_p} = p^n; S^{\nu_s} = S^n$ 
/* outer loop */
while ( pressure equation not converged)
  calculate fine-scale operators;
  update basis functions;
  assemble prolongation operator;
  calculate coarse-scale operators;
  solve for coarse-scale pressure,  $p_c$ ;
  reconstruct dual fine-scale pressure,  $p_d$ ;
  reconstruct primal fine-scale pressure;  $p_v$ ;
   $\nu_p = \nu_p + 1; p^{\nu_p} = p_d$ ;
  update pressure dependent properties:  $b = b(\nu_p)$ ;
  calculate fine-scale total velocity  $\mathbf{u}_T$  from  $p_d$  and  $p_v$ ;
/* inner loop */
while (saturation equation not converged)
  solve linearized transport equation for  $S^{\nu_s+1}$ ;
   $\nu_s = \nu_s + 1$ ;
  update saturation dependent properties:
   $\Rightarrow \lambda = \lambda(S^{\nu_s})$ ;
end
end
 $n = n + 1$ 

```

Figure 3: The pseudo code of OBMM with SFI scheme for one time step

The fine-scale velocity calculated using \mathbf{p}_d may be discontinuous on the interface of dual coarse blocks, since the basis functions assure flux continuity only in the interior region of each dual block. To obtain a conservative fine-scale velocity, we solve the fine-scale Eq.2 locally for each primal coarse block with flux boundary conditions. The flux boundary conditions are obtained from \mathbf{p}_d . The fine-scale pressure computed in this manner, which we denote as \mathbf{p}_v , is the primal fine-scale pressure. Then, the fine-scale velocity in the interior regions of primal coarse blocks is calculated from \mathbf{p}_v , while velocity on the boundary of the primal coarse block is calculated from \mathbf{p}_d . Compressibility is taken into account in the fine-scale fluxes naturally when the fine-scale pressure is available.

Coupling of Flow and Transport. We choose the sequential fully implicit (SFI) algorithm to solve the coupled flow and transport equations. For each time step, in an outer loop we solve for the fine-scale pressure using OBMM and calculate the fine-scale total velocity, \mathbf{u}_T ; in an inner loop we solve for the fine scale saturation implicitly according to Eq.5. The pseudo code for one time step is listed in Fig.3, where n denotes a time step and ν denotes an iteration step.

Note that for the FVM-based OBMM, the restriction operator need to be constructed once as shown by Eq.17. Also note that when solving the saturation equations in the inner loops, the total velocity \mathbf{u}_T is fixed.

Adaptive Updating of Basis Functions The OBMM would not be very efficient if we have to update the basis functions every iteration by solving Eq.7. Jenny et al.^{6,7} proposed adaptive updating of the basis functions according to the change of

total mobility. Namely, if the condition

$$\frac{1}{1 + \epsilon_\lambda} < \frac{\lambda_t^\nu}{\lambda_t^{\nu-1}} < 1 + \epsilon_\lambda \quad (23)$$

is not satisfied for all fine cells inside a dual coarse block, then the basis functions associated with that dual block should be recomputed. The parameter ϵ_λ is a user defined adaptivity threshold.

Although the adaptivity criterion, Eq.23, is proposed for incompressible flow, it also works well for compressible flow. Taking $\epsilon_\lambda < 0.2$ yields results very close to those without adaptivity, and the fraction of basis function that must be recomputed is usually less than 1%.

Numerical Results

We study two-dimensional cases here. The permeability field is extracted from the top layer of the SPE 10 model³. We modified the original permeability field slightly. The extreme low and high values that account for less than 2.5% are clipped. The variance of the logarithmic permeability of this model is $\sigma_{lnk}^2 = 5.04$ (the original variance is 5.45) as shown in Fig.4. It is still a highly heterogeneous model. The fine-scale grid contains 220×60 cells and the coarse-scale grid contains 20×12 blocks. The upscaling factor is 55 (11×5). The field is initially saturated with phase 2 at a uniform pressure. We then begin to inject pure phase 1 in the upper left primal coarse block and produce in the lower right primal coarse block. The production and injection rates are constant in each fine cell within the primal coarse injection and production blocks. Quadratic relative permeability curves are used. The viscosity ratio of the two phases is 1 : 10. The porosity is constant at 0.3.

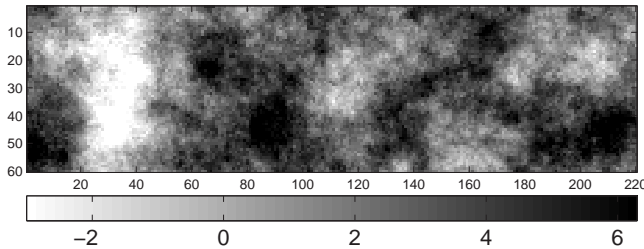


Figure 4: Log-permeability of the top layer of the SPE 10 model

Incompressible Flow. We first study incompressible flow using OBMM. We take the solutions given by fine-scale computation as the reference. Then, we compare the OBMM solutions of the fine-scale pressure, saturation, and horizontal component of total velocity for $t = 0.2$ PVI with the reference solutions. Figures 5 and 6 show that the pressure and velocity field calculated from OBMM are in close agreement with the reference results. Moreover, the match of fine-scale saturation between OBMM and the reference is excellent as shown in Fig.7. The fine-scale saturation error contours are shown in Fig.8, which illustrates that the error is concentrated in a few fine cells around the saturation front.

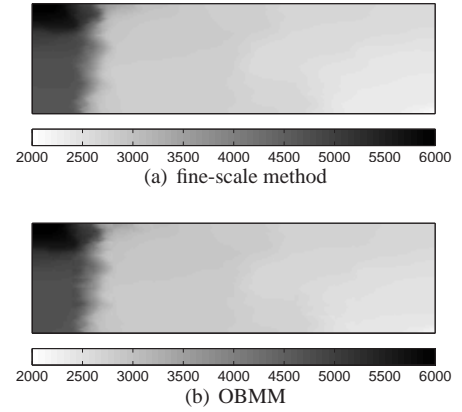


Figure 5: Fine-scale pressure at $t = 0.2$ PVI for the incompressible case

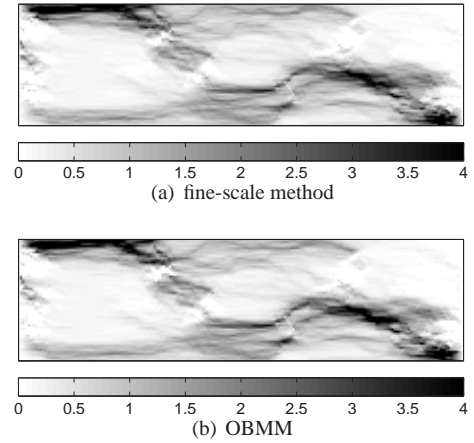


Figure 6: Fine-scale velocity (horizontal component) at $t = 0.2$ PVI for the incompressible case

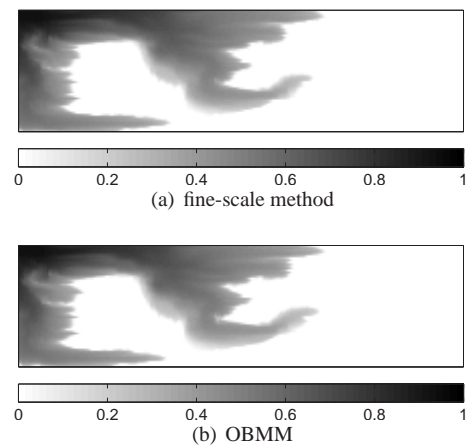


Figure 7: Fine-scale saturation at $t = 0.2$ PVI for the incompressible case

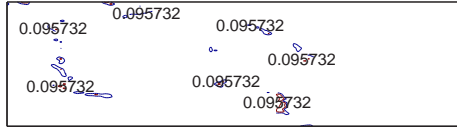


Figure 8: Contours of saturation error at $t = 0.2$ PVI for the incompressible case

The recovery and the production fractional flow of phase 2 are shown in Fig.9. The excellent agreement with the reference solution suggests that OBMM is very accurate for the incompressible case. This is consistent with the findings using the MsFVM⁵.

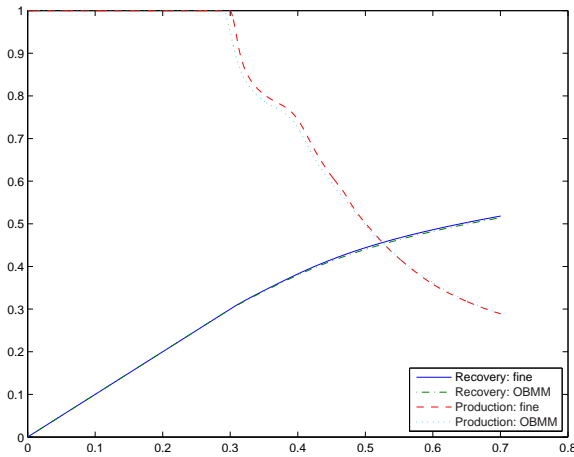


Figure 9: Recovery and production fractional flow of phase 2 for the incompressible case

We report the error statistics and the percentage of basis functions that are recomputed for several time steps in Table 1. The pressure error, ϵ_p , and saturation error, ϵ_s , are defined by

$$\begin{aligned} \epsilon_p &= \frac{\|p^{ms} - p^f\|_2}{\|p^f\|_2}, \\ \epsilon_s &= \|S^{ms} - S^f\|_2, \end{aligned} \quad (24)$$

where superscript f and ms , denote, respectively, the reference and OBMM solutions. f_p denotes the percentage of recomputed basis functions. The overall quality of the OBMM solution is remarkable. The percentage of recomputed basis functions is very small, which leads to efficient computation of highly detailed models.

t (PVI)	ϵ_p	ϵ_s	f_p (%)
0.1	2.07e-2	2.21e-4	0.082
0.2	2.77e-2	2.10e-4	0.041
0.5	3.05e-2	2.03e-4	0.033
0.7	3.55e-2	1.94e-4	0.026

Table 1: Errors and percentage of the recomputed basis functions in several time steps for the incompressible case

Compressible Flow. We consider a highly compressible flow problem. Assume phase 1 is a gas phase satisfying the ideal gas law. Phase 2 is a compressible liquid (oil-like) phase. The PVT properties are given by

$$\begin{aligned} b_1 &= \frac{p}{p_0}, \\ b_2 &= 1 + 10^{-3}(p - p_0), \end{aligned} \quad (25)$$

where p_0 is pressure at standard conditions (14.7 psi).

The OBMM solutions are compared with reference solutions at $t = 0.2$ PVI. From Fig.10, we can see that the pressure variation is large. Thus, we can expect that the effects of compressibility will be very important. For this highly compressible and strongly heterogeneous case, the fine-scale pressure obtained using OBMM is in good agreement with the reference solution. The fine scale velocity in OBMM is also in excellent agreement with the reference as shown in Fig.11. The saturation solution of OBMM is almost identical to the reference solution as shown in Fig.12. This is confirmed by the fine-scale saturation error contours in Fig.13. The recovery and production fractional flow curves obtained using OBMM and the reference solution are shown in Fig.14, which shows that the results are in very close agreement.

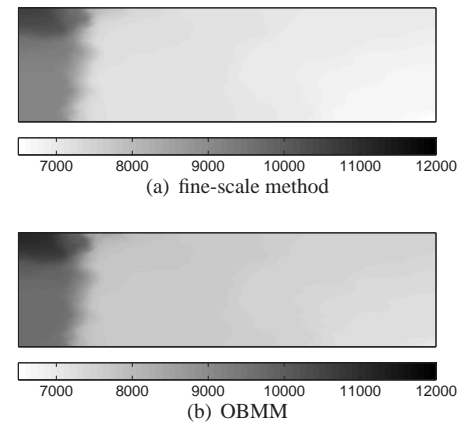


Figure 10: Fine-scale pressure at $t = 0.2$ PVI for the compressible case

Table 2 reports the pressure and saturation errors as well as the percentage of recomputed basis function for each time steps. The quality of the saturation using OBMM is excellent, while the pressure solution shows larger errors compared with incompressible case. Recall that our basis functions are obtained by solving local elliptic problems. In this strongly compressible case, the effect of the parabolic part of the governing equation on the pressure distribution is significant. Thus, the basis functions are less accurate than in the incompressible case. Nevertheless, the compressibility in this case is extreme and the pressure error is still quite reasonable. As shown in Table 2, the percentage of recomputed basis function is higher than that in the incompressible case, but it is still small.

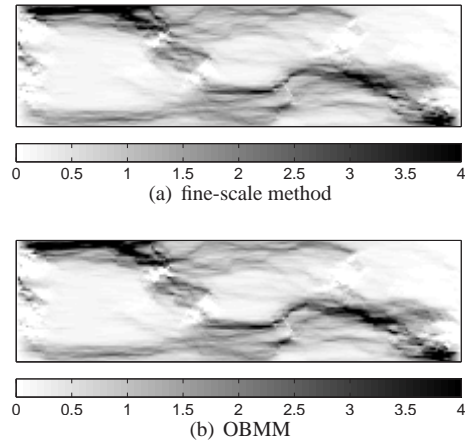


Figure 11: Fine-scale velocity (horizontal component) at $t = 0.2$ PVI for the compressible case

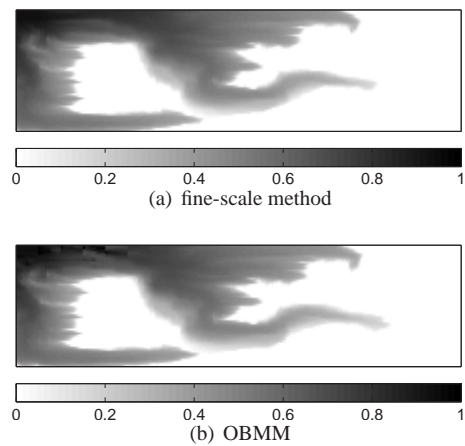


Figure 12: Fine-scale saturation at $t = 0.2$ PVI for the compressible case

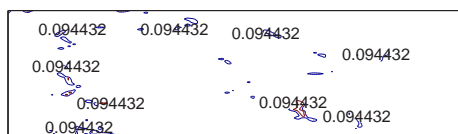


Figure 13: Contours of the saturation error at $t = 0.2$ PVI for the compressible case

t (PVI)	ϵ_p	ϵ_s	f_p (%)
0.1	6.98e-2	2.32e-4	0.15
0.2	6.88e-2	2.43e-4	0.82
0.5	7.60e-2	2.29e-4	0.42
0.7	8.10e-2	2.27e-4	0.31

Table 2: Errors and percentage of the recomputed basis functions in several time steps for the compressible case

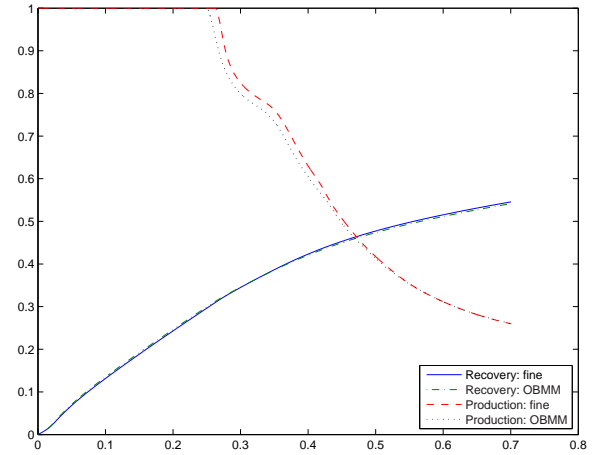


Figure 14: Oil cut and recovery curves for the compressible case

Conclusions

An operator based multiscale method (OBMM) has been developed. OBMM serves as a general algebraic multiscale framework. The prolongation operator is assembled from the basis functions. The restriction operator depends on the chosen discretization scheme. We have shown the restriction operators based on a finite volume method (FVM) and the Galerkin finite element method.

For the incompressible flow problem, the coarse-scale operator constructed by the FVM-based OBMM is identical to the multiscale finite-volume method. OBMM accounts for compressibility effects in a natural way. The fine-scale operators contain the fine-scale compressibility information and the basis functions are calculated with compressibility effects. The coarse-scale operators constructed by OBMM account for compressibility by summing all the fine-scale information in a coarse block and distributing the contribution to the coarse nodes according to the basis functions.

For coupled flow and transport problems, a conservative fine-scale velocity field is crucial. A conservative velocity field is reconstructed by solving Neumann problems locally on the primal coarse blocks. A sequential fully implicit scheme is used to solve the coupled equations.

Test cases for both incompressible and compressible flow are presented, and the results obtained by OBMM are in very good agreement with the reference solutions. The permeability field in the test cases is highly heterogeneous. In the compressible flow case, the compressibility is high and the pressure variation is very large. Such challenging features show that OBMM is reliable in solving highly compressible and strongly heterogeneous problems.

The efficiency of OBMM relative to standard fine-scale methods lies in the fact that we do not solve a global fine-scale system. Constructing and solving the coarse-scale equations takes little computational effort compared with solving the global fine-scale system. Adaptive updating of the basis functions can lead to great efficiency gains. OBMM is readily extendible to more complicated physics. Moreover, it does not depend on explicit description of grid geometry and can be directly applied to

unstructured models. OBMM is purely algebraic and makes full use of the fine-scale properties and equations. Thus, OBMM can be implemented in existing reservoir simulators relatively easily. Compared with building a multiscale simulator from scratch, that will save a great deal of effort.

Acknowledgment

The authors gratefully acknowledge financial support from the members of the affiliate program of the Stanford University Petroleum Research Institute for Reservoir Simulation (SUPRI-B).

References

1. T. Arbogast. Implementation of a locally conservative numerical subgrid upscaling scheme for two-phase darcy flow. *Computational Geosciences*, 6:453–481, 2002.
2. T. Arbogast and S. L. Bryant. A two-scale numerical subgrid technique for waterflood simulations. *SPE Journal*, 7:446–457, 2002.
3. M. A. Christie and M. J. Blunt. Tenth SPE comparative solution project: A comparison of upscaling techniques. *SPE Reservoir Eval. & Eng.*, 4:308–317, 2001.
4. T. Hou and X. H. Wu. A multiscale finite element method for elliptic problems in composite materials and porous media. *Journal of Computational Physics*, 134:169–189, 1997.
5. P. Jenny, S. H. Lee, and H. A. Tchelepi. Multiscale finite-volume method for elliptic problems in subsurface flow simulation. *Journal of Computational Physics*, 187:47–67, 2003.
6. P. Jenny, S. H. Lee, and H. A. Tchelepi. Adaptive multiscale finite-volume method for multiphase flow and transport in porous media. *Multiscale Modeling and Simulation*, 3:50–64, 2004.
7. P. Jenny, S. H. Lee, and H. A. Tchelepi. Adaptive fully implicit multiscale finite-volume method for multiphase flow and transport in heterogeneous porous media. *Journal of Computational Physics*, 217:627–641, 2006.
8. I. Lunati and P. Jenny. Multiscale finite-volume method for compressible multiphase flow in porous media. *Journal of Computational Physics*, 216(2):616–636, 2005.
9. Hui Zhou. Operator based multiscale method for compressible flow. Master's thesis, Stanford University, 2006.